2. V. I. Nikolaev, V. A. Nemtsev, and L. N. Shegidevich, Izv. Akad. Nauk BSSR, Ser. Fiz.-Énerg. Nauk, No. 1, 43-48 (1987).
3. V. B. Nesterenko, Physicochemical and Thermophysical Properties of Chemically Reacting System $N_2O_4 = 2NO_2 = 2NO + O_2$ [in Russian], Minsk (1976).
4. O. Zenkevich, Finite-Element Method in Engineering [in Russian], Moscow (1975).

COMPARISON OF PHYSICAL AND NUMERICAL MODELING OF SUPERSONIC FLOW OVER A CONE

P. A. Voinovich, Yu. P. Golovachev,
I. M. Dement'ev, A. N. Mikhalev,
E. V. Timofeev, and A. A. Fursenko

UDC 519.6:533.6.011.5

Results of a multiapproach study of flow of ideal and viscous gases over conical bodies are evaluated. The experiments were performed with a ballistic device using interferometry.

Interest in the study of supersonic flow over various bodies has been stimulated by this phenomenon's many technological applications. An analytical approach is ineffective because of the significant nonlinearity of the problem and complexity of the flow structures. Initial attempts must involve experiment and numerical methods. Their combined use permits conclusions as to the accuracy and reliability of both measurements and the numerical methods for this class of problems. The present study will compare shock wave contours, gas dynamic function profiles in the shock layer sections, and values of the drag coefficient C_X. A comparison of experimental and calculated values of pressure and thermal flux on the surface of a blunt cone was performed previously [1, 2].

1. The physical experiment was performed with the large ballistic apparatus of the Ioffe Physicotechnical Institute [3]. To obtain optical patterns a diffraction shear interferometer [4] with field of view 200 × 300 mm was used. The light source used was an OGM-20 ruby laser with pulse energy of 0.2 J and pulse length of 30 nsec. Two separate matte scatterers were installed ahead of the condenser in the device illuminator. The laser light was transmitted to the receiver section by a lightguide.

The model of the composite cone (base diameter D = 30 mm) had a velocity V_∞ = 885 m/sec, with Mach number M_∞ = 2.57. The path was filled with air under atmospheric conditions, with Reynolds number as determined by incident flow parameters and diameter of the model base $Re_\infty = 1.12 \cdot 10^6$.

In performing the experiments together with the interferograms direct shadow photographs of the object were obtained in a parallel beam in 10 sections of the device in each of two orthogonal directions. Such a recording of the trajectory allowed measurement of the parameters of model motion and calculation of integral aerodynamic characteristics based thereon [4]. The shadow photographs were also used to determine the position of the head shock wave and the internal waves which develop at the breakpoints of the body directrix. The geometry and centering method chosen insured high stability of the model flight, with attack angle not exceeding 1° over the entire path length. This angle was not considered in the density calculations.

The uncertainty in determining path length difference in the given inhomogeneity did not exceed 0.2-0.3 bands. This value served to establish the statistical dispersion of the density. Using the standard Abel procedure, the distributions of path length difference were used to calculate density profiles in the selected sections.

The drag coefficient C_X was calculated by the method of [5]. For comparison to the resistance coefficient obtained by integration of the calculated pressure and friction forces over the frontal and lateral surface of the model, it is necessary to subtract from C_X the

A. F. Ioffe Physicotechnical Institute, Academy of Sciences of the USSR, Leningrad.
Translated from Inzhenerno-Fizicheskii Zhurnal, Vol. 55, No. 2, pp. 209-212, August, 1988. Original article submitted March 23, 1987.

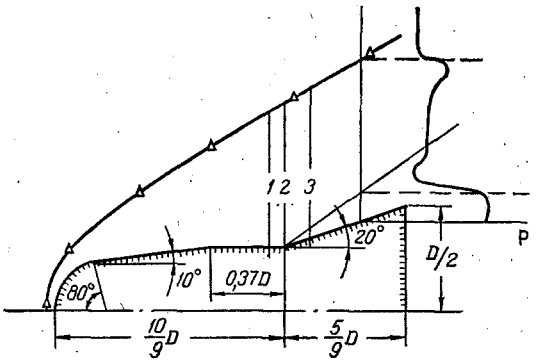

Fig. 1. Meridional section of body flowed over: P, radial pressure profile in tail section: 1, 2, 3) density interpretation sections.

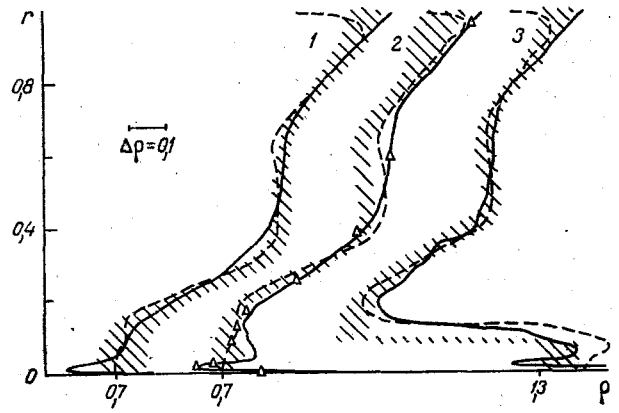

Fig. 2. Density profiles in sections 1, 2, 3 (Fig. 1): r) radial coordinate normalized to the departure of the main wave; ρ) density referenced to ρ_∞.

contribution of bottom resistance. For this purpose use was made of the universal expressions of [6], which agree well with bottom pressure measurements for a cone of similar geometry [7].

2. The numerical studies were performed using the models of an ideal and a viscous gas. The solution of the Euler equations in the blunted region were found by the reconstruction method [8]. From the gas dynamic function fields thus obtained initial data were extracted for calculation of the flow along the side surface of the body. These calculations were performed by a stepped method analogous to that of [9], with automatically conservative smoothing of the solution [10]. A system of simplified (parabolized) Navier–Stokes equations [11] was used to describe motion of the viscous gas in the shock layer. The calculation method used was also of a composite nature. In the blunted region the reconstruction method was used [11], while on the lateral surface of the body the step method was employed [1]. In the vicinity of the compression angle to consider the effect of perturbation propagation up the flow global iterations were performed over the pressure field [12] using smoothing [10]. All these methods have a second order approximation in both spatial coordinates, with the exception of the step method for the viscous gas, which is first order in the longitudinal coordinate.

Calculations were performed for flow over the model of a biatomic ideal gas. In the viscous gas model it was assumed that $\mu \sim \sqrt{T}$, with body temperature surface equal to the temperature of the incident flow.

3. Figure 1 shows the wave structure of the supersonic flow over the composite cone. The solid lines indicate contours of shock waves as determined by optical shadow pictures. The triangles denote the position of the departing shock wave, calculated for its separation. Regarding the calculated pressure profile, one can note the good coincidence of the regions of maximum pressure gradients with the measured positions of the head and internal shock

waves. The calculated value of the lateral resistance coefficient differs from the experimental value of 0.334 by not more than 5%.

Figure 2 shows a comparison of measured and calculated density distributions in sections close to the breakoff of the cone directrix. The hatched lines are data from processing of interferograms, indicating the statistical dispersion of the dimensionless density. It should be noted that in the vicinity of the shock waves an intense packing of the interference bands occurs, leading to a decrease in the accuracy with which their coordinates are determined. In these regions, as well as near the body surface, the resolving power of the experiment did not permit determination of flow structure details.

Results of calculations for the ideal and viscous gas models are shown in Fig. 2 by dashed and continuous lines respectively. Some divergence in the "nonviscous" part of the shock wave can be explained by the use of different difference grids and a different method for calculation of the head shock wave region (its separation in the viscous gas model and indirect calculation in the ideal gas model). As is evident from Fig. 2, consideration of viscous energy dissipation in the viscous gas model leads to a nonmonotonic change in density near the cone surface. Since quantitative comparison with experimental data for this region is not possible, the calculations of the viscous shock layer were performed on a uniform difference grid, the step of which under the conditions considered ($Re_\infty \simeq 10^6$) greatly exceeds the boundary layer thickness. Therefore the density profiles presented in Fig. 2 give only a qualitative representation of the structure of the near-wall region.

Over the greater portion of the shock layer the calculated density profiles agree satisfactorily with the optical measurement data. The difference between the experimental and numerical results does not exceed 6%.

In the profile for section 2 there is an elevation in the density on the external edge of the boundary layer, indicating generation of an internal compression discontinuity. This result was obtained in the viscous gas model with consideration of perturbation propagation up the flow in the compression angle region with the aid of global iterations over the pressure field. The points indicate density values calculated with the viscous gas model by the step method, which insures stable calculation only to section 2.

Thus the observed quantitative correspondence of the measured and calculated values indicates the satisfactory accuracy and reliability of the numerical methods and experiments. A combination of these approaches allows expansion of the range of data obtained and increase in data reliability.

NOTATION

r, coordinate (measured along normal to body axis from surface); D, diameter of model base; ρ, density; μ, dynamic viscosity coefficient; T, absolute temperature; V, gas velocity; M, Mach number; Re, Reynolds number; C_x, drag coefficient. Subscript ∞, unperturbed flow.

LITERATURE CITED

1. Yu. P. Golovachev and A. A. Fursenko, Zh. Vychisl. Mat. Mat. Fiz., 21, No. 6, 1592-1596 (1981).
2. P. A. Voinovich, Yu. P. Golovachev, and A. A. Fursenko, Numerical Methods in Viscous Liquid Dynamics. Proceedings of the IX All-Union School-Seminar [in Russian], Sib. Otd. Akad. Nauk SSSR, Novosibirsk (1983), pp. 90-95.
3. I. V. Basargin, I. M. Dement'ev, and G. I. Mishin, Aerophysical Studies of Supersonic Flows [in Russian], Moscow–Leningrad (1967), pp. 168-178.
4. I. A. Belov, I. M. Dement'ev, S. A. Isaev, et al., "Modeling supersonic flow over bodies of rotation with leading breakoff zone," Preprint A. F. Ioffe Fiz. Tekh. Inst., No. 1033 [in Russian] (1986).
5. N. P. Mende, Physico-Gas Dynamic Ballistic Studies [in Russian], Leningrad (1980), pp. 200-224.
6. R. F. Starr, Raket. Tekh. Kosmon., 15, No. 5, 171-173 (1977).
7. Yu. V. Shelud'ko, Physico-Gas Dynamic Ballistic Studies [in Russian], Leningrad (1980), pp. 68-77.
8. A. N. Lyubimov and V. V. Rusanov, Gas Flow About Blunt Bodies [in Russian], Vol. 1, Moscow (1970).
9. A. V. Ricci, E. Klavins, and R. W. MacCormack, News in Foreign Science, Mechanics, No. 14 [in Russian], Moscow (1977), pp. 121-143.

10. A. I. Zhmakin and A. A. Fursenko, Zh. Vychisl. Mat. Mat. Fiz., 20, No. 4, 1021-1031 (1980).
11. Yu. P. Golovachev and F. D. Popov, Zh. Vychisl. Mat. Mat. Fiz., 12, No. 5, 1292-1303 (1972).
12. P. A. Voinovich and A. A. Fursenko, Diff. Uravn., 20, No. 7, 1151-1156 (1984).

THERMAL BURST IN THE FLOW OF NONLINEARLY VISCOUS MEDIA THROUGH A ROUND TUBE

Yu. G. Nazmeev, V. A. Minenkov, and A. I. Mumladze

UDC 532.135

The problem of critical thermal conditions in a structurally viscous liquid flowing through an infinite tube is solved numerically with an allowance for the combined action of chemical and mechanical heat sources.

The thermal burst occurring during an exothermic chemical reaction in a medium at rest, which is characterized by a progressive temperature rise, was predicted and described in [1]. It has been shown in [2-4] that a phenomenon similar to a thermal burst can occur in the flow of a chemically inert, "exponential" liquid in an infinite tube or the flow of reactive Newtonian media whose viscosity is heavily dependent on the temperature.

We shall investigate the thermal burst in the laminar, axisymmetric flow of a generalized, structurally viscous, incompressible, and reactive liquid with an allowance for the combined action of chemical and dissipative heat release.

We assume that the thermophysical characteristics of the liquid are constant, a zero-order reaction is in progress, and a constant temperature is maintained at the tube wall. Then, the system of equations of motion and energy conservation with an allowance for dissipative heat release and heat release due to the chemical reaction has the following form:

$$\frac{\partial \tau}{\partial r}+\frac{\tau}{r}=\frac{\partial P}{\partial z}=\text{const},\ r\in(0,\ r_1), \tag{1}$$

$$\lambda\left(\frac{\partial^2 T}{\partial r^2}+\frac{1}{r}\frac{\partial T}{\partial r}\right)+\tau\frac{\partial v}{\partial r}+Q_0k_0\exp\left(\frac{-E}{RT}\right)=0,\ r\in(0,\ r_1) \tag{2}$$

with the boundary conditions

$$\text{for } r=0\ \tau=0,\ \partial T/\partial r=0, \tag{3}$$

$$\text{for } r=r_1\ v=0,\ T=T_0=\text{const}. \tag{4}$$

As a rheological model, we shall use the Kutateladze–Khabakhpasheva equation [5] for a structurally viscous liquid,

$$\varphi_*=\exp(-\tau_*), \tag{5}$$

where $\varphi_*=(\varphi_\infty-\varphi)/(\varphi_\infty-\varphi_0)$ and $\tau_*=\Theta|\tau-\tau_0|/(\varphi_\infty-\varphi_0)$.

Since viscosity is a more complex function of the shearing stress than fluidity, which is the inverse quantity [5], the phenomenological theory of liquid flow with structural viscosity has been developed with respect to $\varphi(\tau)$, which is, for $\tau > \tau_0$, defined in the one-dimensional case as

$$dv/dr=-\varphi(\tau-\tau_0),\ r\in(r_0,\ r_1). \tag{6}$$

We represent the temperature relationships of the rheological model parameters in the Arrhenius form:

$$\varphi_0=A_0\exp(-B/RT),\ \varphi_\infty=A_\infty\exp(-B/RT), \tag{7}$$

$$\Theta=\Theta_0\exp(-B/RT),\ \tau_0=a_0\exp(-b_0(T-T_0)).$$

Kazan Branch, Moscow Power Institute. Translated from Inzhenerno-Fizicheskii Zhurnal, Vol. 55, No. 2, pp. 212-217, August, 1988. Original article submitted April 3, 1987.

 0022-0841/88/5502-0858$12.50